Influence of the laser source position on the generation of Rayleigh modes in a layer–substrate structure with varying degrees of adhesion

Martin Robin, Frédéric Jenot, Mohammadi Ouaftouh, Marc Duquennoy

Influence of the laser source position on the generation of Rayleigh modes in a layer–substrate structure with varying degrees of adhesion

Martin Robin, Frédéric Jenot, Mohammadi Ouaftouh, Marc Duquennoy

Univ. Polytechnique Hauts-de-France, CNRS, Univ. Lille, YNCREA, Centrale Lille, UMR 8520 – IEMN – Institut d'Électronique de Microélectronique et de Nanotechnologie, DOAE – Département d'Opto-Acousto-Électronique, F-59313 Valenciennes, France

Corresponding author:

Frédéric Jenot :
frederic.jenot@uphf.fr
Université Polytechnique Hauts-de-France
IEMN-DOAE
Campus Mont Houy
F-59313 Valenciennes, France

Non-Destructive Testing of adhesion using Surface Acoustic Waves (SAW) is an important issue in industrial and academic domains. Indeed, these waves are sensitive to the quality of adhesion at the interface between the substrate and the layer with a thickness comparable to the acoustic wavelength. Furthermore, their propagation distance allows a large majority of the sample to be tested quickly. Numerous studies have used SAW for the Non-Destructive Testing of adhesion. However, some recurrent experimental difficulties may lead to an incorrect interpretation of the results. This is the case when the layer thickness is non-uniform, for example. To provide a quasi-constant thickness, a PolyEthylene Terephthalate (PET) film was placed directly on the substrate surface without any glue and Laser-Ultrasonics was used to investigate this type of structure. As the film was transparent at the optical wavelength used, it was possible to focus the laser source on the substrate surface through the film. To the best of our knowledge, no paper has been published on the influence of the source position on adhesion testing. In this work, two source positions were investigated.

Keywords: Adhesion, Non-Destructive Testing, Surface Acoustic Waves, Laser-Ultrasonics, Wigner-Ville distribution

1. Introduction

Thin films are used in numerous industrial domains such as microelectronics to modify the surface properties of layer-substrate structures. The lifetime of these coatings is directly linked to the quality of adhesion at the interface and so it is very useful to develop a Non-Destructive Testing method to characterize the adhesion.

Surface Acoustic Waves (SAW) are well suited to this purpose. For the structures considered, the SAW become dispersive and are known as Rayleigh modes. The contact conditions at the interface influence this dispersion. Laser-Ultrasonics was chosen for its ability to generate and detect acoustic waves without requiring contact as well as for its large frequency bandwidth [1]–[3].

Numerous studies have been published about adhesion testing using acoustic waves, but many concern bulk waves [4]. Most of the papers dealing with SAW focus on piezoelectric transducers to excite and detect these waves [5], [6]. Only a few deal with laser sources among which a limited

number of studies concerns the influence of adhesion on SAW dispersion curves [7]–[15]. Most of these studies mention the difficulties in linking the variations in the dispersion to the adhesion due to variations in layer thickness [11], [12] and the unknown mechanical characteristics of the glue layer [7], [10], [14], [15]. In these studies, only optically opaque samples are considered.

To avoid these problems, a PolyEthylene Terephthalate (PET) film was deposited on an aluminum substrate. The variations in the thickness of this layer are very small in comparison with typical coatings and the film can be stuck to the substrate surface without any glue. Moreover, it is optically transparent at the laser wavelength ($532\ nm$), so Rayleigh modes can be generated directly on the substrate at the interface by focusing the laser pulse through the film. Consequently, the influence of the acoustic source position on the surface waves dispersion according to the variations in the degree of adhesion can be investigated.

In the first part, we investigate the influence of variations in thickness and adhesion on the Rayleigh mode dispersion curves. The Matrix Transfer method by Thomson-Haskell was used to establish the dispersion relation [16], [17]. The well known interfacial stiffness method was used to model the influence of adhesion on acoustic waves propagation [18]–[20].

In the second part, Finite Element simulations taking the position of the source into account are presented.

Finally, the experimental results are discussed and compared to the theoretical predictions. Different degrees of adhesion were considered and their influence on acoustic wave propagation was analyzed using a laser source located at the interface.

2. Analytical study

SAW dispersion phenoma depends on the layer and substrate materials, which are assumed to be isotropic in this case. Depending on the shear wave velocities of the film and the substrate, it is possible to observe three types of dispersive behavior [21]. In our case, the ratio between the shear wave velocity in the film $c_T{}'$ and in the substrate c_T is less than $1/\sqrt{2}$, as shown in Table 1. In this situation, several Rayleigh modes, which the phase velocity decreases with the frequency, propagate in the structure. At low frequencies, the first mode tends to the Rayleigh wave velocity in the substrate, and higher order modes tend to the shear wave velocity in the substrate because the wavelength is long in relation to the film thickness. At high frequencies, the first mode tends to the Rayleigh wave velocity in the film and higher order modes tend to the shear wave velocity in the film. Indeed, for these frequencies, the acoustic wavelength is small compared to the film thickness [21].

These observations are only valid in the case of perfect contact, which is given by:

$$\begin{cases} \sigma'_{ij} = \sigma_{ij} \\ u'_i = u_i \end{cases} \quad (1)$$

where σ_{ij} is the stress in the substrate at the boundary ($\sigma_{ij}{}'$ is the stress in the film at the boundary) in the direction i to the surface of normal j and u_i is the particle displacement in the substrate at the boundary ($u_i{}'$ is the particle displacement in the film at the boundary) in the direction i.

The most commonly used model in the literature represents the interface as a very thin layer compared to the acoustic wavelength. Adhesion depends on its mechanical characteristics [20]. In addition, considering that its mass is negligible, it is possible to approximate the interface with a normal and a tangential stiffness, denoted by K_n and K_t [20], respectively. The boundary conditions are then given as follows:

$$\begin{cases} \sigma'_{ij} = \sigma_{ij} \\ \sigma_{ij} = K_m(u'_i - u_i) \end{cases} \quad (2)$$

where $K_m = K_n$ for the normal component to the interface (i.e. $i = j$), and $K_m = K_t$ for the tangential component to the interface (i.e. $i \neq j$).

Table 1 summarizes the characteristics used to calculate the dispersion curves presented on Figure 1 to 3. These values were measured experimentally using bulk waves generated by piezoelectric transducers and the pulse-echo method. The film thickness ($h = 132\ \mu m\ \pm 1.5\ \%$) was obtained using a high-precision comparator.

	PET film	**Aluminum substrate**
Longitudinal wave velocity $(\boldsymbol{m/s})$	1950	6400
Shear wave velocity $(\boldsymbol{m/s})$	1000	3140
Thickness $\boldsymbol{h}$	$132\ \mu m$	$10\ cm$
Density $(\boldsymbol{kg/m^3})$	1350	2798

Table 1: Characteristics of the materials used for the analytical calculations and the simulations.

Table 2 presents the stiffness values used to determine the dispersion curves. The higher K_n and K_t, the greater the adhesion is. Values higher or lower than quasi-perfect contact and quasi-total disbanding, respectively, were not considered. Indeed, values outside these limits no longer have a significant influence on the dispersion curves. These values were chosen arbitrarily.

Degree of adhesion	**Normal stiffness** $\boldsymbol{K_n}$ $(\boldsymbol{N/m^3})$	**Tangential stiffness** $\boldsymbol{K_t}$ $(\boldsymbol{N/m^3})$
Perfect contact	∞	∞
1 (quasi-perfect contact)	2.10^{16}	1.10^{16}
2	6.10^{13}	3.10^{13}
3	2.10^{13}	1.10^{13}
4	2.10^{12}	1.10^{12}
5 (quasi-total disbonding)	2.10^{8}	1.10^{8}
Total disbonding	0	0

Table 2: Stiffness values used to model adhesion for the analytical calculations and the simulations.

Figure 1 shows the influence of adhesion on the dispersion curves of the Rayleigh modes for a PET film on an aluminum substrate structure, calculated using the matrix transfer method [16], [17]. The dispersion curves corresponding to the degrees of adhesion 1 and 5 overlap with those for perfect contact and total disbanding, respectively. The solid lines represent perfect contact (black) and total disbonding (green and red). In the latter situation, one curve corresponds to the Rayleigh wave propagating in the substrate (green) and the other one to Lamb waves propagating in the film (red). The dashed lines represent intermediate degrees of adhesion (2 cyan, 3 magenta and 4 blue). The weaker the adhesion is, the more the dispersion curves tend to those for the Rayleigh and Lamb waves in the substrate and the film, respectively. In this case, the first two Rayleigh modes clearly tend to the first two Lamb modes in the film. With weak degrees of adhesion, the third Rayleigh mode tends to the Rayleigh wave in the substrate for the low-frequency part. However, at high frequencies, this mode tends to the third Lamb mode in the film. The third and fourth Rayleigh modes exhibit the opposite behavior. Figure 2 clearly shows this evolution for the degrees of adhesion 3 (top figure) and 5 (middle figure), as well as the Lamb modes in a PET film and the Rayleigh wave in an aluminum substrate (bottom figure).

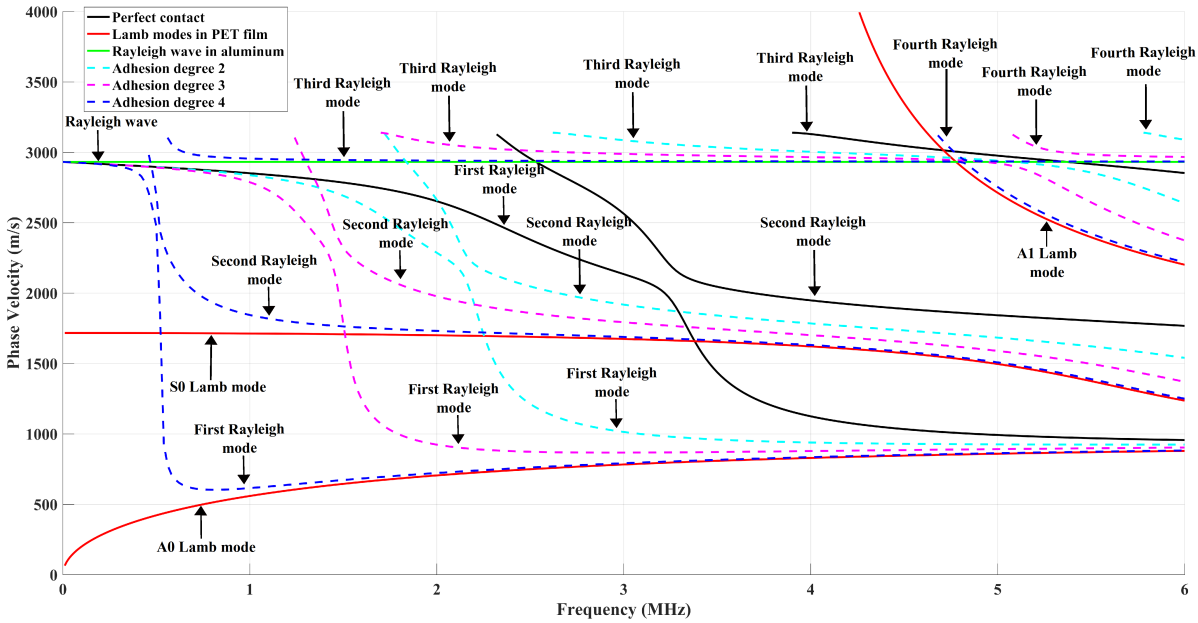

Figure 1: Rayleigh modes dispersion curves in a PET-aluminum structure for different degrees of adhesion.

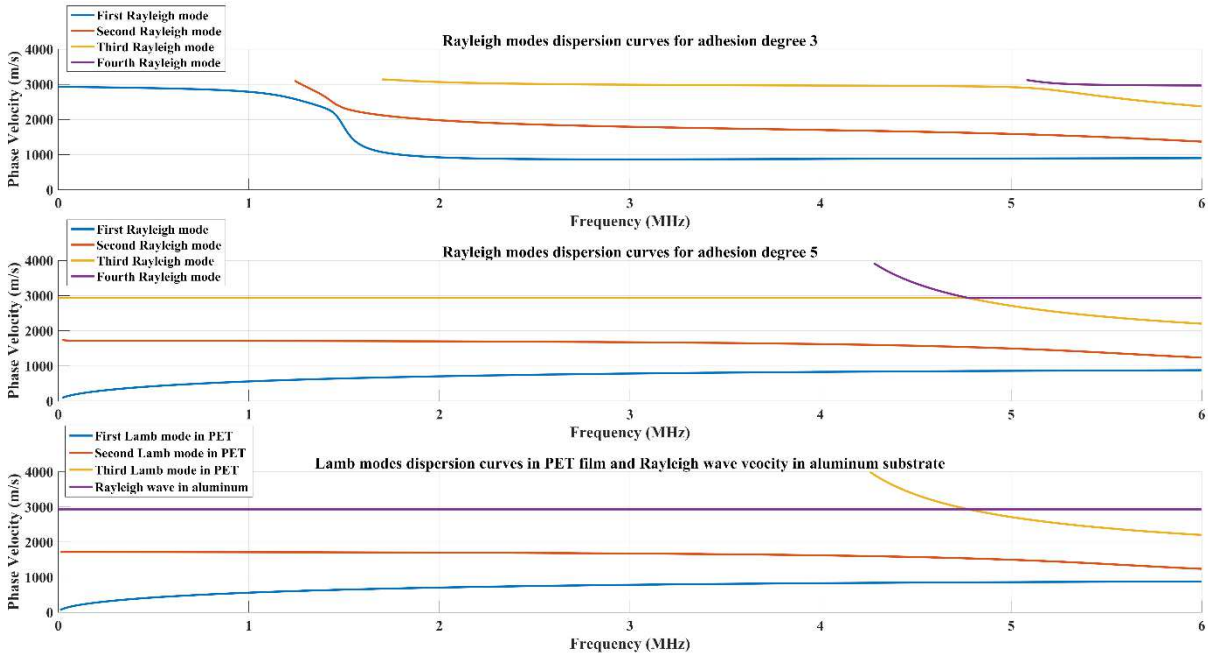

Figure 2: Rayleigh modes dispersion curves in a PET-aluminum structure for degree of adhesion 3 (top figure), degree of adhesion 5 (middle figure) and Lamb modes in PET film and Rayleigh wave in an aluminum substrate (bottom figure).

This result is original because it brings an additional contribution to articles published concerning the evolution of Rayleigh modes towards Lamb waves in the film [5], [14]. The analytical calculation carried out does not consider the source position. Two types of Rayleigh mode behaviors were obtained for weak adhesion but only one of these was observed depending on the position of the source. In the case of poor adhesion, when the source is located in the film or at its surface, the dispersion curves tend to those of guided waves in the coating, whereas when the acoustic source is located on the substrate, the Rayleigh modes become a Rayleigh wave.

The film thickness also influences the dispersion curves depending on the quality of adhesion. Figure 3 presents the dispersion curves of the first two Rayleigh modes for different film thicknesses and contact conditions. As shown, the results obtained with small variations in adhesion are similar to those obtained with small variations in thickness. In order to avoid this problem, we have chosen a layer-substrate structure with a quasi-constant thickness.

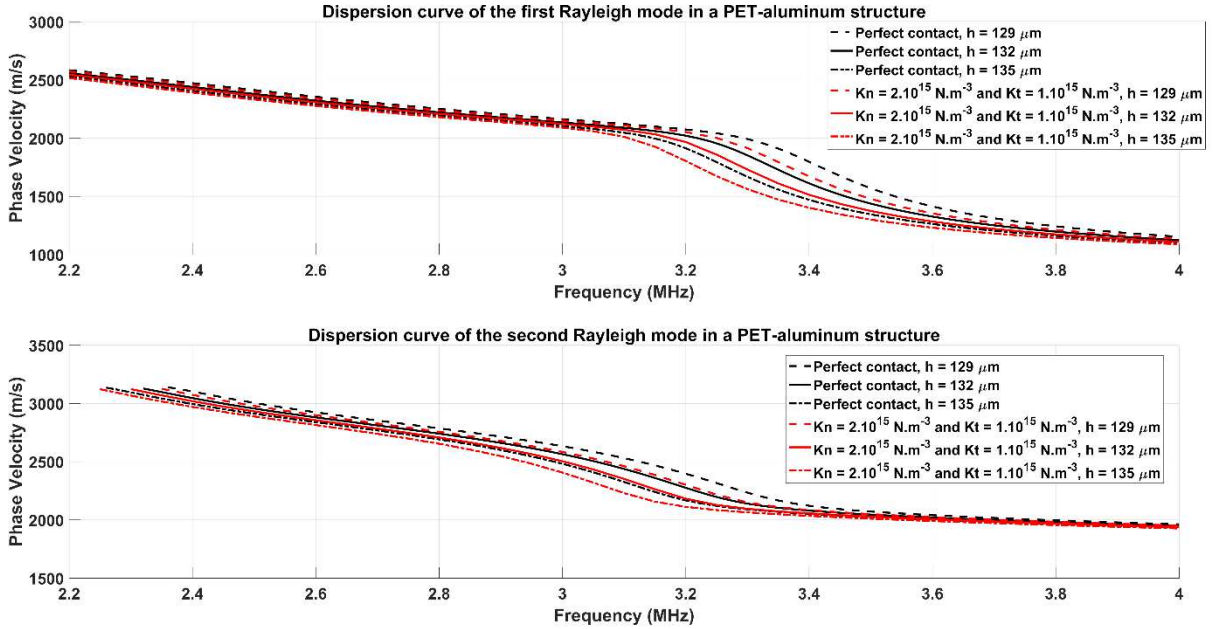

Figure 3: Dispersion curves of first (top figure) and second (bottom figure) Rayleigh modes in PET–aluminum structure with different values of thickness for the PET film and different degrees of adhesion.

3. Finite Element Modeling

To study the influence of the source position, Finite Element simulations were conducted using the COMSOL Multiphysics software [3]. The quality of the adhesion between the film and the substrate was modeled by considering the interface as a thin layer $100\,nm$ thick. Its mechanical characteristics were determined using the stiffness values given in Table 2 [20].

The source for generating the acoustic waves was modeled using a tangential forces dipole at the film surface or at the interface. The normal displacement of the acoustic waves was measured using 201 point probes with an interval of $50\,\mu m$.

Two configurations were investigated. The source and the probes were placed at the film-substrate interface (on the substrate surface) in the first configuration (Figure 4 a) and on the film surface in the second case (Figure 4 b). For each configuration, simulations were carried out for the 5 degrees of adhesion summarized in Table 2. The elastic parameters used for the two materials are those given in Table 1.

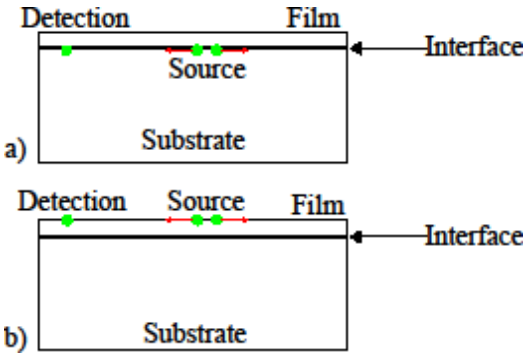

Figure 4: Source and detection positions for the two configurations studied.

A 2D Fast Fourier Transform was applied to the probe signals to obtain the Rayleigh modes phase velocity dispersion curves. Figure 5 shows the results for the 5 degrees of adhesion in the first configuration. The results corresponding to the second configuration are presented in Figure 6. The colormap corresponds to the normalized modulus of the Fast Fourier Transform. The solid line represents the previous dispersion curves obtained from the analytical calculations. For the fifth degree of adhesion, the analytical curves correspond to the Rayleigh wave in the substrate (Figure 5) and Lamb modes in the film (Figure 6).

Figure 5 and 6 clearly highlight the influence of the source position on the modes generated. When the excitation is at the interface on the substrate side (Figure 5), the first four Rayleigh modes are clearly observed, as expected. The second mode only appears for very good adhesion and disappears for bad adhesion. The low-frequency part of the first mode is generated for all degrees of adhesion except total disbonding. When adhesion decreases, a shift in the dispersion curve to lower-frequencies is observed. Only the low-frequency part of the third mode and the high-frequency part of the fourth mode exist for all the degrees of adhesion considered. Whatever the degree of adhesion, only the parts of the dispersion curves around the Rayleigh wave velocity in the substrate are generated. This also explains why the second mode is more difficult to excite when adhesion decreases. Indeed, its part around the Rayleigh wave velocity in the substrate is reduced due to a steeper slope.

When the acoustic source is placed on the film surface, the opposite phenomenon is observed. This time, the first and second modes are predominant and their excited parts correspond to phase velocities that are lower or higher than the Rayleigh wave velocity in the substrate. When adhesion decreases, these modes tend to the first two Lamb modes in the film. The third and fourth Rayleigh modes are weakly excited with good degrees of adhesion and only the high-frequency part of the third mode and the low-frequency part of the fourth mode are excited when adhesion is weak. These two modes merge together to form the third Lamb mode in the film.

These results show that each mode is composed of a combination of a Rayleigh wave part and a Lamb mode part. For a given source position, only one of these two parts is excited. When adhesion decreases, this part tends to Rayleigh wave in the substrate when the source is placed at the interface, or tends to Lamb modes in the film when the source is placed at the surface of the film. These simulations confirm our assumption stated previously following the analytical calculations. Only one of the two configurations is observed for a given source location when adhesion is very weak.

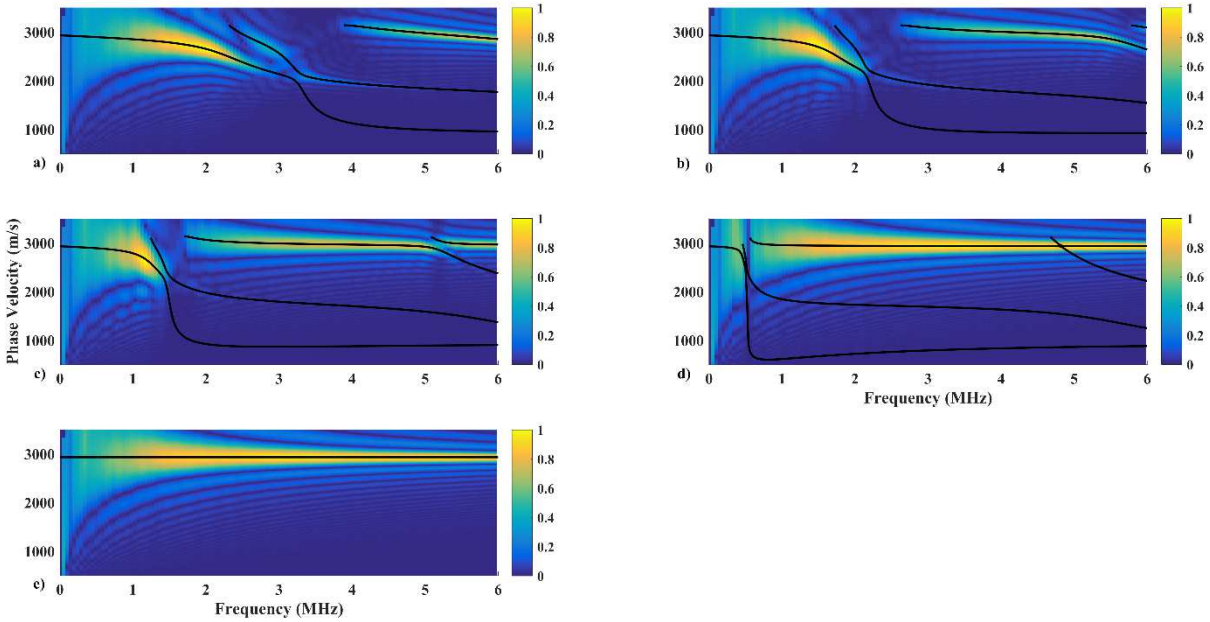

Figure 5: Dispersion curves obtained from the FEM simulations with source and probes placed between the layer and the substrate at the interface. a) to e): Degrees of adhesion 1 to 5. Black curves correspond to analytical calculations.

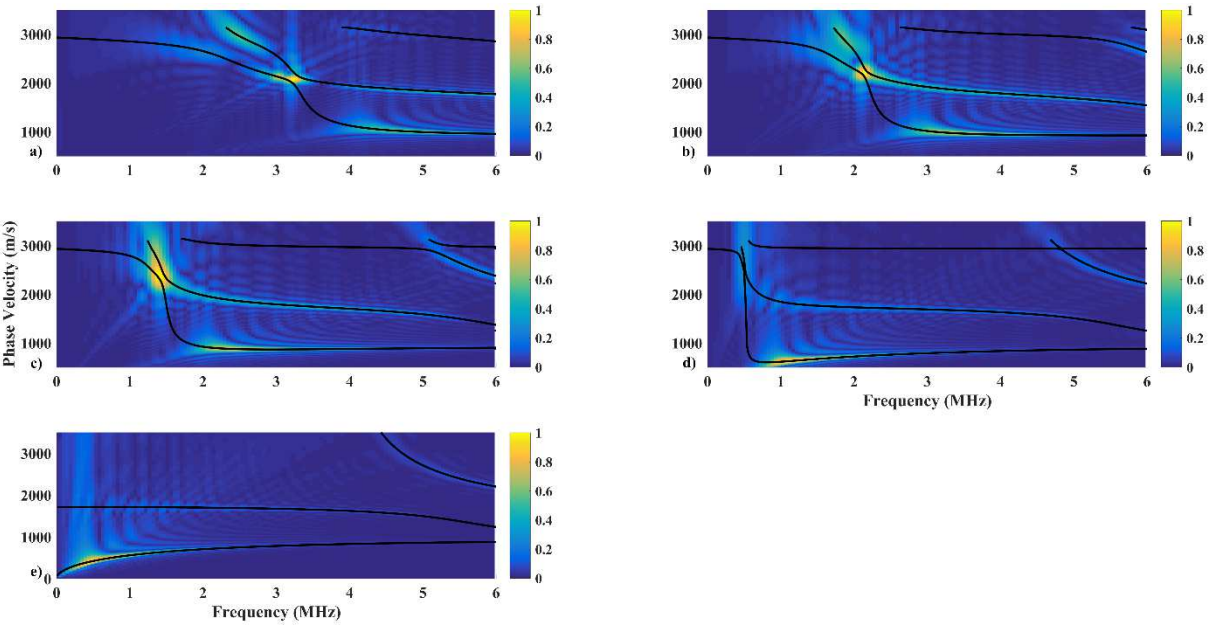

Figure 6: Dispersion curves obtained from the FEM simulations with source and probes placed on the film surface. a) to e): Degrees of adhesion 1 to 5. Black curves correspond to analytical calculations.

4. Experimental study

a. Measurement setup

The samples used were composed of a PET film in direct contact with an aluminum substrate. It was possible to remove and replace the film several times before adhesion was no longer possible.

Figure 7 shows the experimental setup. A $10\ ns$ Q-switched Nd:YAG laser pulse of $532\ nm$ was focused as a line source on the aluminum substrate surface, through the PET film.

The normal displacement of the surface waves was detected by a Mach-Zehnder type interferometer with a power of $100\,mW$ and a bandwidth of $200\,kHz - 45\,MHz$. To improve sensitivity, a filter with a bandwidth of $200\,kHz - 4\,MHz$ was used. To improve the signal-to-noise ratio, eight laser shots were performed for each measurement. Detection was achieved directly on the substrate surface, away from the film.

To vary the adhesion, Polytetrafluoroethylene (PTFE) particles were sprayed on the side of the film in contact with the substrate. These particles are known to be anti-adherent. The film was removed from the substrate between two experiments to add PTFE in order to progressively decrease the adhesion. In this way, the variations in surface wave propagation observed experimentally were mainly due to the contact conditions between the film and the substrate.

Four degrees of adhesion were achieved using different grids (see Figure 8) to protect the film to a lesser or greater extent when the PTFE was sprayed on. The greater the surface area covered with PTFE, the weaker the adhesion is.

The first degree of adhesion corresponds to good adhesion when there is no PTFE on the film. For the other degrees of adhesion, PTFE was sprayed on the film starting with the grid with the smallest holes and ending with the grid with the largest holes.

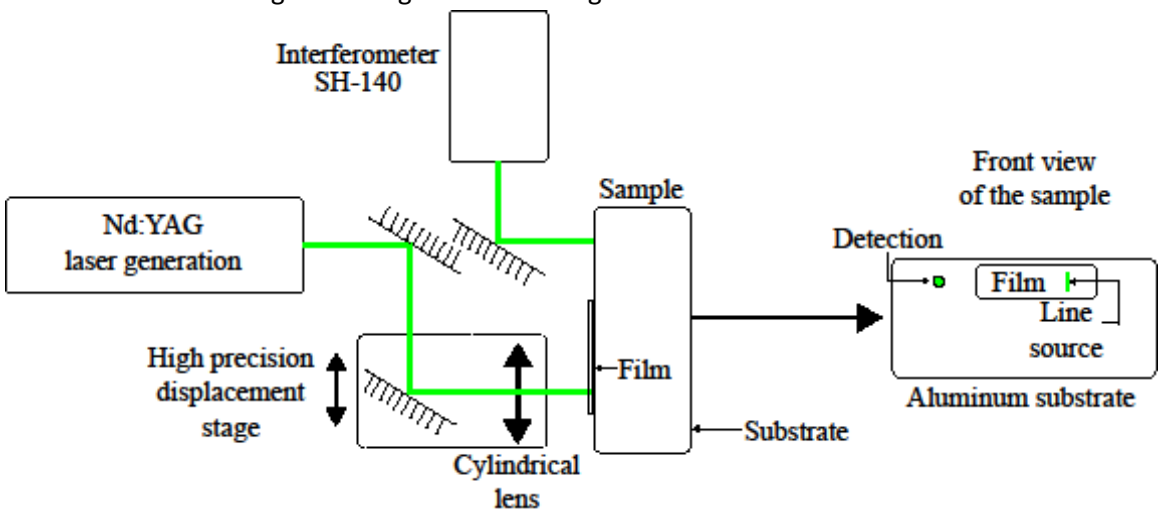

Figure 7: Laser-Ultrasonics setup.

A smoothed pseudo-Wigner-Ville distribution was applied to the signals obtained, which provides a good time-frequency representation of the latter [22]–[24].

Only the generation and detection at the interface between the substrate and the film was investigated here. Indeed, the configuration of a source-probe position at the film surface has already been considered in other studies on opaque films [5].

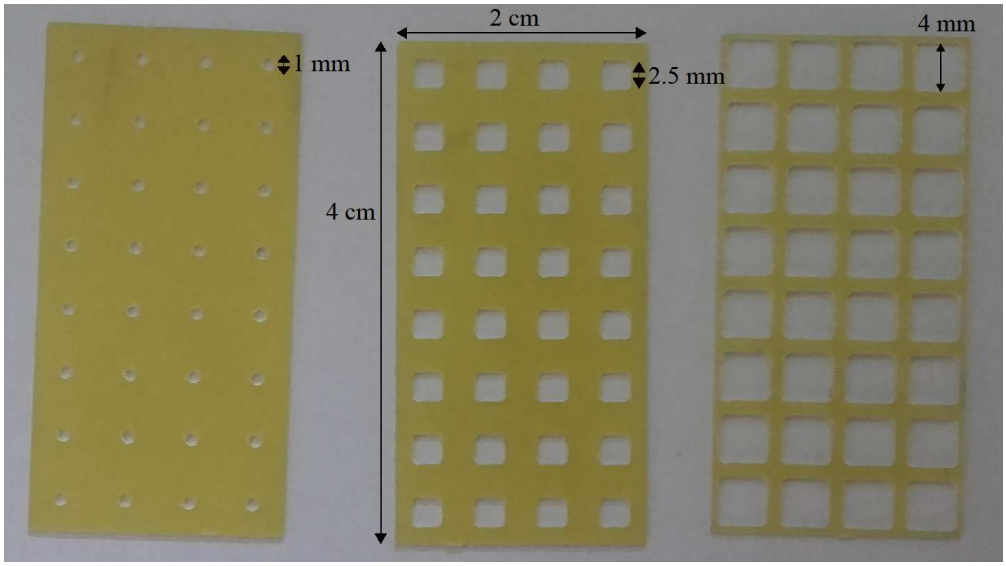

Figure 8: Grids used to mask the film when the PTFE is sprayed. The left grid allows a weak PTFE covering of the surface and the right grid a large one.

b. Experimental results

Figure 9 presents the signals obtained for the different configurations. Figure 9 a corresponds to the signal obtained for the film with no PTFE. Figure 9 b to 9 d correspond to the signals obtained with PTFE sprayed through the three grids from left to right, respectively (Figure 8). Figure 9 e was obtained for the substrate alone to simulate a total disbonding.

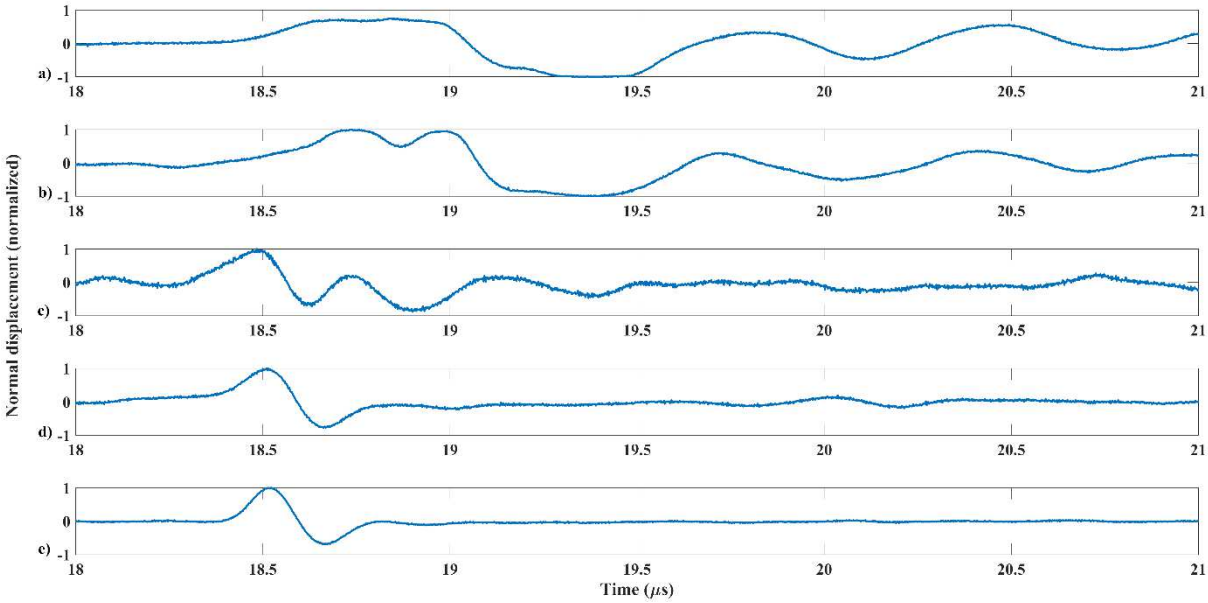

Figure 9: Signals corresponding to the five configurations. a: Without PTFE, b to d: With PTFE using grid from left to right (Figure 8), e: Considering substrate without film.

Figure 9 clearly shows that the weaker the adhesion, the less dispersive the signal is. With complete disbonding the latter becomes a Rayleigh wave in the substrate (Figure 9 e). Figure 9 a and 9 b are similar due to the small holes in the grid used. The signal in Figure 9 d is very close to the Rayleigh wave signal despite the presence of the film over the substrate corresponding to very bad adhesion. These results are in good agreement with the simulation results provided previously.

Figure 10 presents the smoothed pseudo-Wigner-Ville distributions linked to the signals in Figure 9. The colormap corresponds to the normalized square modulus of the Wigner-Ville distribution.

As mentioned before, Figures 10 a and 10 b are similar and clearly dispersive. The frequency band and the dispersive nature of the signals indicate that the first Rayleigh mode is observed, as shown in Figures 5 a, 5 b or 5 c.

Figure 10 d and 10 e exhibit non-dispersive waves as expected from the simulation results in Figures 5 d or 5 e.

Figure 10 c presents a slightly dispersive part at low frequency. Above $1.5\ MHz$, non-dispersive components appear at a velocity close to that of the Rayleigh wave. This behavior is similar to that observed in Figure 5 c.

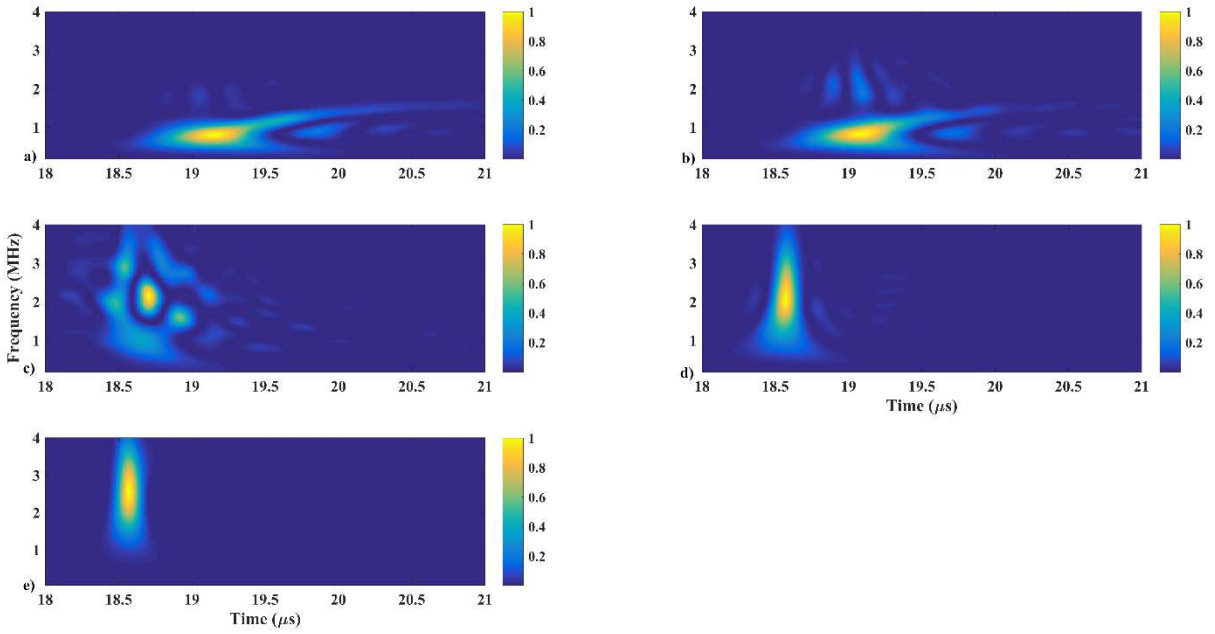

Figure 10: Normalized square modulus of the smoothed pseudo-Wigner-Ville distribution for the signals shown on Figure 9. a: Without PTFE, b to d: With PTFE using grid from left to right (Figure 8), e: Considering substrate without film.

5. Conclusion

This work deals with the influence of the source position on SAW in film-substrate structures with varying degrees of adhesion. Analytical calculations, Finite Element simulations, and experiments were conducted to investigate this. Using a transparent PET film in combination with Laser-Ultrasonics, we were able to generate acoustic waves at the interface. Furthermore, the small variations in the thickness of the film made it possible to consider that the changes in Rayleigh modes behavior were mainly due to adhesion.

We have clearly shown that for different degrees of adhesion, the Rayleigh modes behavior depends on the source position. Two configurations were considered. The first one corresponded to an excitation located at the interface. In this case, the weaker the adhesion, the closer the Rayleigh mode behavior was to that of the Rayleigh wave in the substrate. For the second configuration, the source was placed on the surface of the film. In this case, the Rayleigh modes tended to the Lamb modes in the film as adhesion decreased.

To characterize adhesion, it would be interesting to combine interface excitation with generation at the surface of the film. This would be very useful to obtain more information and resolve the inverse problem with greater accuracy.

References

[1] J. Sermeus, B. Verstraeten, R. Salenbien, P. Pobedinskas, K. Haenen, et C. Glorieux, « Determination of elastic and thermal properties of a thin nanocrystalline diamond coating using all-optical methods », *Thin Solid Films*, vol. 590, p. 284-292, Sept. 2015.

[2] F. Faëse, F. Jenot, M. Ouaftouh, M. Duquennoy, et M. Ourak, « Laser-ultrasound-based non-destructive testing-optimization of the thermoelastic source », *Measurement Science and Technology*, n° 26, 2015.

[3] S. Fourez, F. Jenot, M. Ouaftouh, M. Duquennoy, et M. Ourak, « Non-contact thickness gauging of a thin film using surface waves and a void effect on their propagation », *Measurement Science and Technology*, vol. 23, n° 8, p. 085608, Aug. 2012.

[4] M. Grossmann *et al.*, « Characterization of thin-film adhesion and phonon lifetimes in Al/Si membranes by picosecond ultrasonics », *New Journal of Physics*, vol. 19, n° 5, p. 053019, May 2017.

[5] J. Du, B. R. Tittmann, et H. S. Ju, « Evaluation of film adhesion to substrates by means of surface acoustic wave dispersion », *Thin Solid Films*, vol. 518, n° 20, p. 5786-5795, Aug. 2010.

[6] P. Puthillath et J. L. Rose, « Ultrasonic guided wave inspection of a titanium repair patch bonded to an aluminum aircraft skin », *International Journal of Adhesion and Adhesives*, vol. 30, n° 7, p. 566-573, Oct. 2010.

[7] S. Mezil, F. Bruno, S. Raetz, J. Laurent, D. Royer, et C. Prada, « Investigation of interfacial stiffnesses of a tri-layer using Zero-Group Velocity Lamb modes », *The Journal of the Acoustical Society of America*, vol. 138, n° 5, p. 3202-3209, 2015.

[8] X. Xiao, Y. Sun, et X.-M. Shan, « Nondestructive determination of interfacial adhesion property of low-k/Si by the surface acoustic waves », *Surface and Coatings Technology*, vol. 207, p. 240-244, Aug. 2012.

[9] X. Xiao, H. Qi, Y. Tao, et T. Kikkawa, « Study on the interfacial adhesion property of low-k thin film by the surface acoustic waves with cohesive zone model », *Applied Surface Science*, vol. 388, p. 448-454, Dec. 2016.

[10] A. Abbate, B. Knight, M. A. Hussain, et J. Frankel, « Coating-bond evaluation using dispersion curves and laser-ultrasonics », in *Ultrasonics Symposium, 2000 IEEE*, 2000, vol. 1, p. 721-724.

[11] D. Schneider, H. Ollendorf, et T. Schwarz, « Non-destructive evaluation of the mechanical behaviour of TiN-coated steels by laser-induced ultrasonic surface waves », *Applied Physics A Materials Science & Processing*, vol. 61, n° 3, p. 277-284, Sept. 1995.

[12] H. Ollendorf, D. Schneider, T. Schwarz, et A. Mucha, « Non-destructive evaluation of TiN films with interface defects by surface acoustic waves », *Surface and Coatings Technology*, vol. 74-75, p.
246-252, Sept. 1995.

[13] H. Cho, S. Ogawa, et M. Takemoto, « Non-contact laser ultrasonics for detecting subsurface lateral defects », *NDT & E International*, vol. 29, n° 5, p. 301-306, Oct. 1996.

[14] T.-T. Wu et Y.-Y. Chen, « Wavelet Analysis of Laser-Generated Surface Waves in a Layered Structure With Unbond Regions », *Journal of Applied Mechanics*, vol. 66, n° 2, p. 507, Oct. 1999.

[15] F. Bruno, « Optimisation des modes de Lamb à vitesse de groupe nulle engendrés par laser et évaluation de structures collées », Université Paris Diderot, 2017.

[16] W. T. Thomson, « Transmission of Elastic Waves through a Stratified Solid Medium », *Journal of Applied Physics*, vol. 21, n° 2, p. 89-93, Feb. 1950.

[17] N. A. Haskell, « The dispersion of surface waves on multilayered media », *Bulletin of the seismological Society of America*, vol. 43, n° 1, p. 17-34, 1953.

[18] J. P. Jones et J. S. Whittier, « Waves at a flexibly bonded interface », *J. appl. Mech*, vol. 34, n° 4, p. 905-909, 1967.

[19] M. Schoenberg, « Elastic wave behavior across linear slip interfaces », *The Journal of the Acoustical Society of America*, vol. 68, n° 5, p. 1516-1521, 1980.

[20] S. I. Rokhlin et Y. J. Wang, « Analysis of boundary conditions for elastic wave interaction with an interface between two solids », *Journal of the Acoustical Society of America*, vol. 89, n° 2, p. 503-515, 1991.
[21] G. W. Farnell et E. L. Adler, « Elastic wave propagation in thin layers », in *Physical Acoustics*, vol. 9, Academic Press, Inc., 1971.
[22] P. Flandrin, « Some features of time-frequency representations of multicomponent signals », in *ICASSP '84. IEEE International Conference on Acoustics, Speech, and Signal Processing*, San Diego, USA, 1984, vol. 9, p. 4.
[23] P. Flandrin et B. Escudié, « Principe et mise en oeuvre de l'analyse temps-fréquence par transformation de Wigner-Ville », *Traitement du Signal*, vol. 2, n° 2, p. 143-151, 1985.
[24] J. F. Allard, R. Bourdier, et C. Depollier, « Utilisation de la pseudo-distribution de Wigner-Ville lissée pour la détermination de l'instant de fermeture de la glotte », *Traitement du Signal*, vol. 4, p. 6, 1987.